PHYSICAL REVIEW E **81**, 046109 (2010)

Statistical characterizers of transport in communication networks

Satyam Mukherjee* and Neelima Gupte†
Department of Physics, Indian Institute of Technology, Madras, India

Gautam Mukherjee‡
Bidhan Chandra College, Asansol 713304, Dt. Burdwan, West Bengal, India
(Received 29 August 2009; revised manuscript received 8 March 2010; published 20 April 2010)

We identify the statistical characterizers of congestion and decongestion for message transport in model communication lattices. These turn out to be the travel time distributions, which are Gaussian in the congested phase, and logarithmic normal in the decongested phase. Our results are demonstrated for two-dimensional lattices, such the Waxman graph, and for lattices with local clustering and geographic separations, gradient connections, as well as for a one-dimensional ring lattice with random assortative connections. The behavior of the distribution identifies the congested and decongested phase correctly for these distinct network topologies and decongestion strategies. The waiting time distributions of the systems also show identical signatures of the congested and decongested phases. The distributions are explained using a stochastic differential equation to model the transport.

DOI: 10.1103/PhysRevE.81.046109 PACS number(s): 89.75.Hc

I. INTRODUCTION

Investigations of traffic flows on substrates of various topologies have been a topic of recent research interest [1]. Congestion effects can occur in real networks such as telephone networks, computer networks, and the internet due to various factors such as capacity, bandwidth, and network topology [2]. These lead to deterioration of the service quality experienced by users due to an increase in network load. Congestion and decongestion transitions can be seen in such systems. Statistical characterizers which can identify the state of the network, whether congested or decongested, can be of practical utility. In this paper, we identify statistical characterizers which carry the signature of the state of congestion or decongestion of the network.

The statistical characterizer which carries the signature of the congested or decongested phase is identified to be the travel time distribution of the messages. The travel time distribution has been studied earlier in the context of vehicular traffic [3], server traffic [4] and the internet [5]. Hence the travel time distribution can be regarded as a useful statistical characterizer of transport. In our model networks, the travel time is defined to be the time required for a message to travel from source to target, including the time spent waiting at congested hubs. This distribution turns out to be normal or Gaussian in the congested phase and logarithmic normal in the decongested phase.

We demonstrate that the travel time distribution is able to identify correctly the congested or decongested state in the case of two-dimensional (2D) model networks, such as the Waxman topology network, a popular model for internet topology [6], as well as for a network with local clustering [7], and its variants with gradient connections [8]. The same characterizer is able to distinguish between the congested and decongested phases in a network with one-dimensional (1D) ring geometry. Thus, the travel time distribution is a robust characterizer of the congested or decongested phase. The nature of the distributions can be explained using stochastic differential equations to model the transport.

II. 2D MODEL NETWORKS

We first consider models based on 2D lattices. We note that communication networks based on two-dimensional lattices have been considered earlier in the context of search algorithms [9] and of network traffic with routers and hosts [10,11] and have been observed to reproduce realistic features of internet traffic.

The first network based on a 2D geometry is the Waxman graph [6], which incorporates the distance dependence in link formation which is characteristic of real world networks [12] and has been widely used to model the topology of intradomain networks [13]. We consider the case where the Waxman graphs are generated on a rectangular coordinate grid of side L with the probability $P(a,b)$ of an edge from node a to node b given by

$$P(a,b) = \beta \exp\left(-\frac{d}{\alpha M}\right), \tag{1}$$

where the parameters $0<\alpha, \beta<1$, d is the Euclidean distance from a to b, and $M=\sqrt{2}\times L$ is the maximum distance between any two nodes [6]. Large values of β result in graphs with larger link densities and small values of α increase the density of short links as compared to the longer ones. A topology similar to Waxman graphs is generated by selecting randomly a predetermined number N_w of nodes in the 2D lattice for generating the edges. Additionally, each node of the lattice has a connection to its nearest neighbors [see Fig. 1(a)].

The second network that we study is a model which incorporates local clustering and geographic separations devel-

*mukherjee@physics.iitm.ac.in
†gupte@physics.iitm.ac.in
‡gautamm.krishna@gmail.com

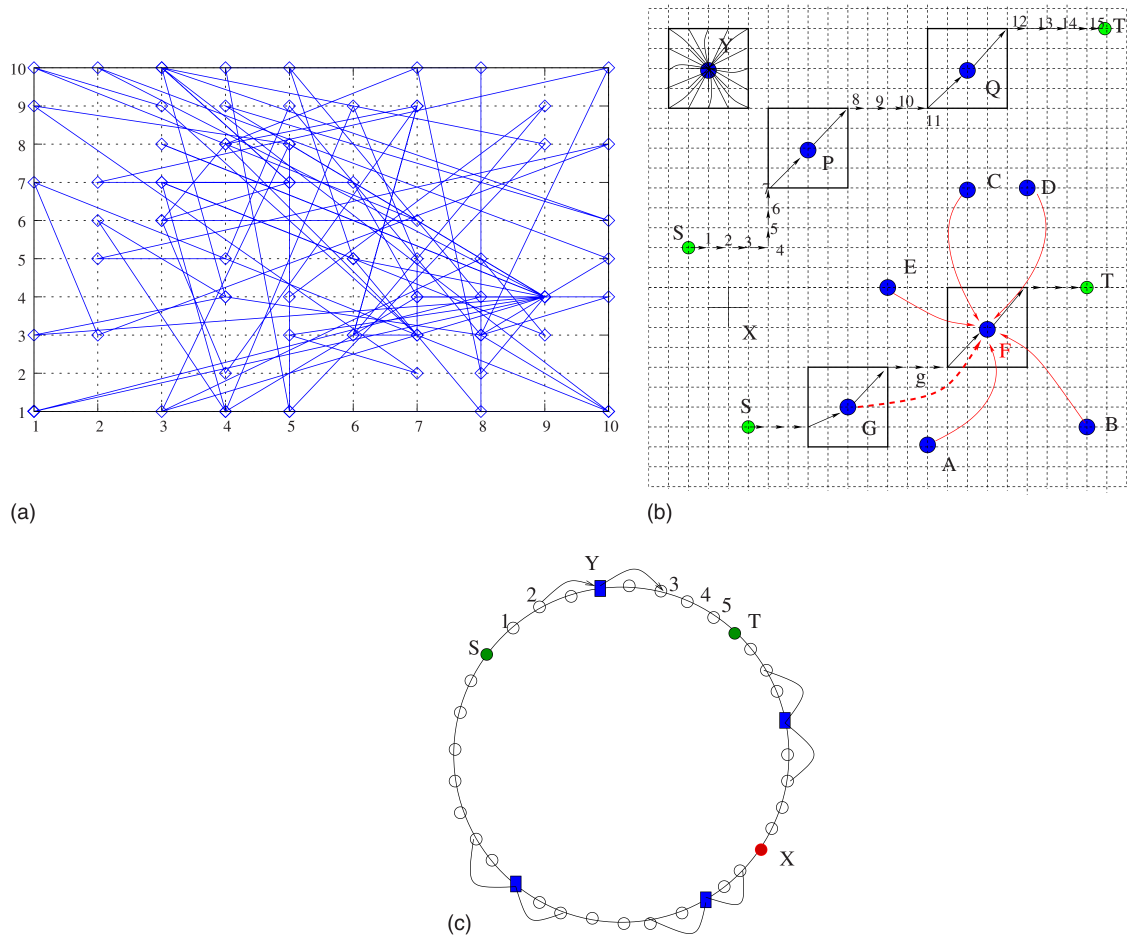

FIG. 1. (Color online) (a) The figure shows a Waxman topology network generated by connecting 55 points by the Waxman algorithm for α=0.05 and β=0.1 on a 10×10 lattice. The number of links increases as the values of α and β are increased. (b) A regular two-dimensional lattice. X is an ordinary node with nearest-neighbor connections. Each hub has a square influence region (as shown for the hub Y). A typical path from the source S to the target T is given by the path S-1-2-3-⋯-7-P-8-⋯-11-Q-12-⋯-T. After the implementation of the gradient mechanism, the distance between G and F is covered in one step as shown by the link g and a message is routed along the path $S-1-2-3-\mathrm{G}-\mathrm{g}-\mathrm{F}-4-5-6-T$. (c) A 1D ring lattice of ordinary nodes (X) with nearest-neighbor connections and randomly distributed hubs (Y).

oped in Ref. [7]. As shown in Fig. 1(b), this network consists of a 2D lattice with nodes and hubs, where the hubs are randomly located on the lattice and are connected to all nodes inside their given area of influence, a square of side $2a$. In our simulation, we set a=3. No two hubs are separated by less than a minimum distance, $d_{\min}$. Here we choose $d_{\min}$=1. For both the Waxman graph and locally clustered 2D network, the distance between a randomly chosen source $S(is,js)$ and target $T(it,jt)$ is given by the Manhattan distance $D_{st}=|is-it|+|js-jt|$. We set free boundary conditions. The message holding capacity of ordinary nodes as well as the hubs is unity. Thus every node (including the hubs) can process one message at a time. The routing algorithm for the messages is described in the next section.

Routing algorithm, congestion, and decongestion

A given number of messages N_m are allowed to travel on these lattices between fixed source target pairs by a distance based routing algorithm. In the case of the clustered lattice, a node which holds a message looks for a hub in the direction of the target which is nearest to itself and routes the message to it [7,8]. Consider a message that starts from the source S and travels toward a target T as shown in Fig. 1(b). The node. which is the current message holder, transfers the message to the node nearest to itself in the direction which minimizes the distance to the target. If the node lies in the influence area of a hub, it sends the message directly to the hub. If the current message holder is a hub, it sends the message to the node or hub, which is connected to itself, and minimizes the distance to the target. For the Waxman network, again the message travels from source to target via nodes which send the message along the connections which minimize the distance to the target. When a message arrives at its target it is removed from the network. As mentioned earlier, the message processing capacity of all hubs and nodes is assumed be unity, and parallel updates are carried out. Therefore, during multiple message transfer, if the would be recipient node or hub is occupied, then the message waits for a unit time step at the current message holder. If the desired

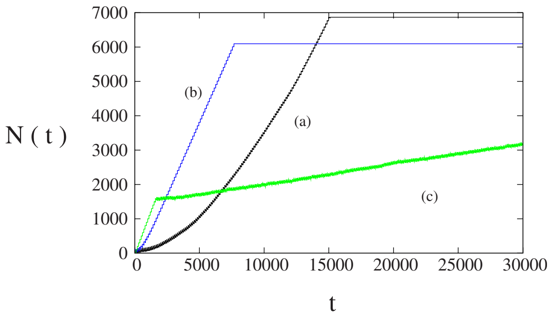

FIG. 2. (Color online) The figure shows the number of messages $N(t)$ flowing on the lattice as a function of time t for (a) the Waxman topology network and the baseline mechanism for (b) the locally clustered 2D lattice and (c) the 1D ring network.

node is still occupied after the waiting time is over, the current node selects any unoccupied node from its remaining neighbors and hands over the message. If all the neighboring nodes are occupied, the message waits at the current message holder until one of them is free.

Clearly, when many messages travel on the network, the finite capacity of the hubs can lead to the trapping of messages in their neighborhoods and a consequent congestion or jamming of the network. Here, we study a situation where N_m messages are deposited at regular intervals on the network. If the message deposition takes place faster than the rate at which messages clear, the network can congest [14]. The numbers of messages $N(t)$ which are flowing on both the 2D lattices as a function of a time t are plotted in Fig. 2. Here, $N_m=100$ messages are deposited every 120th time step for a given run time. For these parameters, the networks get congested and $N(t)$ gets saturated indicating the formation of transport traps as seen in [8]. The reasons for trapping include the opposing movement of messages from sources and targets situated on different sides of the lattice, as well as edge effects.

A variety of decongestion mechanisms can be set up for these lattices. An efficient way of decongesting the clustered lattice has turned out to be the gradient mechanism [8]. This is implemented by identifying the hubs with the five highest values of *CBC* [15], assigning them capacity proportional to their *CBC* values, and setting up a gradient connection to the hub with the highest capacity. Messages can now travel along the gradient connection. The transition to the congested phase occurs for a much larger number of messages (or more frequent rates of deposition), once the gradient strategy is implemented.

The number of messages that are trapped (N_T) on the network for a given posting rate (N_m messages at every Γ time steps) can indicate the level of congestion on the lattice. We plot N_T on the two networks as a function of the number of messages N_m deposited at every $\Gamma=120$, 150, 200, 250 time steps for the baseline mechanism [Fig. 3(a)] and the gradient mechanism [Fig. 3(b)] for run times of 60 000 steps and the Waxman topology network [Fig. 3(c)] for a run time of 90 000 steps, respectively. Here we choose N_m in the range $20 \leq N_m \leq 300$. It is evident that even for smaller values of N_m, the two networks congest if messages are posted at every 120 or 150 time steps. However, a clear decongestion-congestion transition is seen if messages are posted at every 200 or 250 time steps since the number of trapped messages $N_T=0$ if $N_m<100$ indicating a decongested phase for the network. If $N_m>100$ the value of N_T

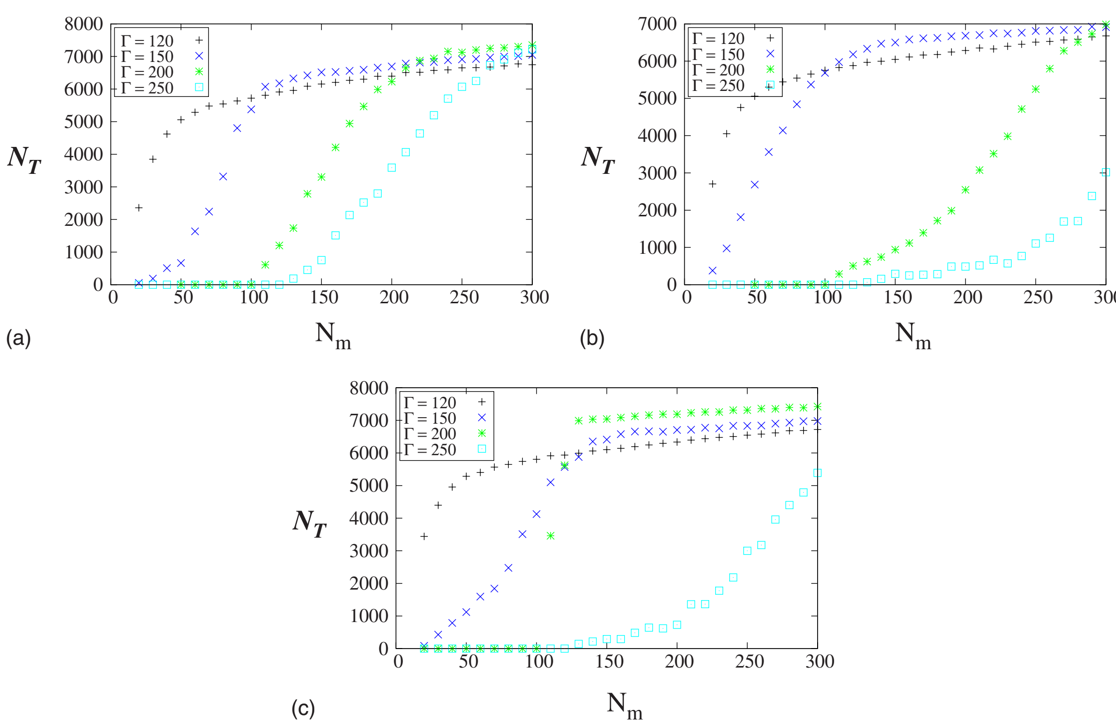

FIG. 3. (Color online) Figure shows the plot of number of trapped messages N_T as a function of the number of N_m messages deposited at every $\Gamma=120$, 150, 200, 250 time steps for (a) baseline and (b) gradient mechanism on locally clustered network and (c) Waxman topology network ($\alpha=\beta=0.05$).

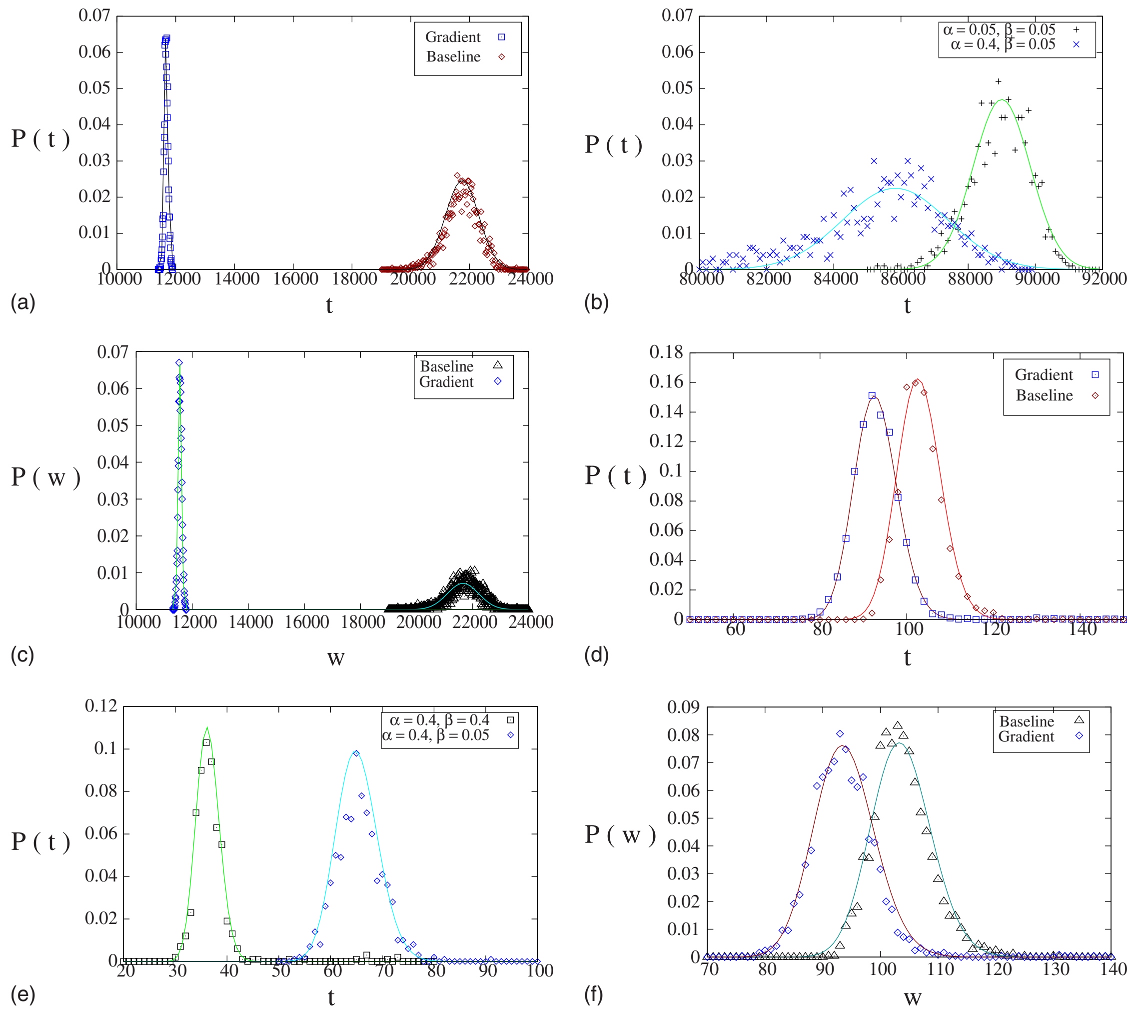

FIG. 4. (Color online) For (a)–(c) the travel time and waiting time distributions in the congested phase shows a Gaussian distribution. For (d)–(f) the distributions change to a logarithmic normal in the decongested phase. The values of σ and χ^2 are given in Table I. Here, (a), (d), (c), and (f) correspond to the network with nodes and hubs, and (b) and (e) to the Waxman networks.

increases and goes toward saturation indicating the congested phase of the network. It should also be noted that for both the congested and decongested regime, the gradient mechanism is more efficient than the baseline mechanism. The number of messages trapped in the gradient mechanism is much less than that of the baseline mechanism for the same values of N_m and Γ.

III. STATISTICAL CHARACTERIZERS OF TRANSPORT

We can now identify the statistical characterizer of the congested and decongested phase for these two networks. This turns out to be the travel time distribution. Here the travel time is the total travel time of messages including the time each message waits on all the nodes to be delivered to adjacent node along the path of their journey to respective targets. For the Waxman topology network if messages are fed on the system at a constant rate of $N_m=100$ messages at every 120 time steps for $N_w=100$ and total run time of 90 000, messages are not delivered to their targets and the network is in the congested phase. For the locally clustered 2D network we allow $N_m=100$ messages be deposited at every 120 time steps on a 100×100 lattice with $D_{st}=142$, for 100 hubs and total run time of 60 000. At this value of N_m many messages remain undelivered in the lattice due to the onset of traps and the system is in the maximal congested regime. The travel time distribution for this congested phase for both these networks is shown in Fig. 4. The travel time distribution can be fitted by a Gaussian of the form

$$P(t)=\frac{1}{\sigma\sqrt{2\pi}}\exp\left(-\frac{(t-\mu)^2}{2\sigma^2}\right). \qquad (2)$$

If 100 messages are fed continuously at every 200 time steps all the messages get delivered to their targets for both cases, and the data for the travel time distribution can be fitted by a logarithmic normal distribution of the form

$$P(t)=\frac{1}{t\sigma\sqrt{2\pi}}\exp\left(-\frac{(\ln t-\mu)^2}{2\sigma^2}\right). \qquad (3)$$

Thus it is evident that during the congested phase the travel time distribution for messages deposited at a constant rate in

TABLE I. The table shows the value of σ and χ^2 for the Fig. 4. Here σ is the standard deviation and χ^2 is the chi-squared test for accuracy of the fit. The third, fourth, and fifth rows correspond to the Waxman graphs at the indicated values of α and β.

Network Models	Congested phase	Decongested phase
Baseline [$P(t)$]	σ=567.31 (χ^2=0.195)	σ=0.113 (χ^2=0.075)
Gradient [$P(t)$]	σ=64.07 (χ^2=0.026)	σ=0.122 (χ^2=0.075)
α=0.05, β=0.05	σ=850.37 (χ^2=0.463)	
α=0.4, β=0.05	σ=1576 (χ^2=0.852)	σ=0.06 (χ^2=0.066)
α=0.4, β=0.4		σ=0.062 (χ^2=0.06)
Baseline [$P(w)$]	σ=560 (χ^2=0.2)	σ=0.056 (χ^2=0.04)
Gradient [$P(w)$]	σ=60 (χ^2=0.02)	σ=0.05 (χ^2=0.04)

the network, shows Gaussian behavior [Figs. 4(a) and 4(b)]. On the other hand log-normal behavior is found during the decongested phase [Figs. 4(d) and 4(e)]. The decongestion-congestion transition occurs at a much higher value once the gradient strategy is implemented. Here again, the decongested phase shows a logarithmic normal distribution of travel times, and the normal phase shows a Gaussian distribution of travel times. The values of σ and χ^2 for the fits in Fig. 4 are shown in Table I. Similar results are seen for other decongesting strategies, such as connecting the hubs of high *CBC* by random assortative connections [7]. The waiting time distribution of the system, where the waiting time is defined to be the time for which the messages wait at congested nodes, also show an identical signature of the congestion-decongestion transition [Figs. 4(c) and 4(f)].

TABLE II. The table shows the value of Γ_c for different values of N_m for the baseline mechanism.

N_m	Γ_c
5	110
10	155
25	165
50	175
75	190
100	200
125	250
150	305
175	390
200	630

A. Phase diagram

The phase diagram of the system can be inferred from the behavior of the plot of the number of messages trapped (N_T) as a function of posting rate. As mentioned earlier, these are plotted for N_m=25, 50, 75, 100, 125 messages (Fig. 5) deposited at regular intervals of Γ time steps ($100 \le \Gamma \le 250$) for the baseline mechanism [Fig. 3(a)], the gradient mechanism [Fig. 3(b)], and the Waxman topology network [Fig. 3(c)], respectively. It is observed that for higher values of Γ the number of trapped messages decreases and N_T=0 for Γ $=\Gamma_c$ and above. The values of Γ_c for different values of N_m, for the baseline mechanism, are listed in Table II.

We use Table II to plot the phase diagram for congestion-decongestion transition for the baseline mechanism in the

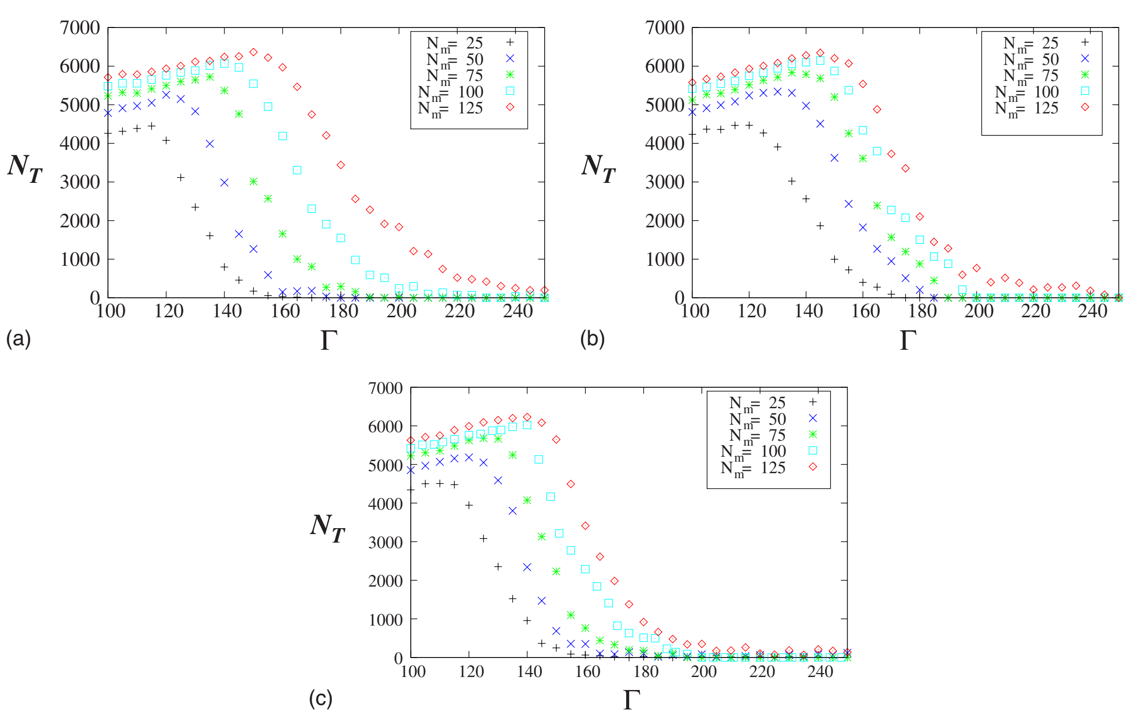

FIG. 5. (Color online) The plot of number of messages trapped on the lattice when N_m=25, 50, 75, 100, 125 messages are deposited at regular intervals of Γ (a) baseline and (b) gradient mechanism on locally clustered network and (c) Waxman topology network ($\alpha=\beta$ =0.05).

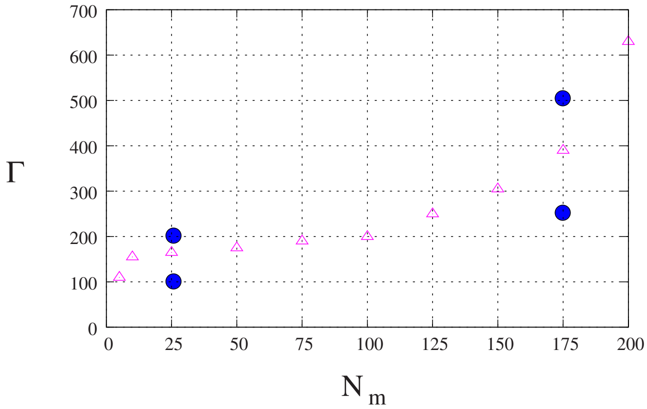

FIG. 6. (Color online) Phase diagram for the congestion-decongestion transition for the baseline mechanism in the locally clustered 2D lattice. Here N_m is the number of messages and Γ is the posting rate. The blue (filled) circles denote the points which are chosen from the congested and decongested phase for evaluation of travel time distributions. The triangles indicate the location of Γ_c for a given N_m.

locally clustered 2D lattice as shown in Fig. 6. Obviously, for a given value of N_m, the system is in the decongested state for values of $\Gamma > \Gamma_c$ and in the congested phase for $\Gamma < \Gamma_c$. The statistical characterizers of the system accurately pick up the phase of the system.

We choose two values of N_m for different values of Γ and evaluate the travel time distribution for these (the points chosen are indicated by solid circles in Fig. 6). It can be seen that for $N_m=25$, $\Gamma=100$ and $N_m=175$, $\Gamma=250$ the system is in the congested phase and the travel time distributions can be fitted by a Gaussian [Fig. 7(a)]. However for $N_m=25$, $\Gamma=200$ and $N_m=175$, $\Gamma=500$ the system attains decongestion and the travel time distributions show logarithmic-normal behavior [Fig. 7(b)]. Thus, the travel time distributions carry the signature of congestion or decongestion. Similar phase diagrams can be constructed for the Waxman and gradient cases as well, with similar results.

B. 1D ring lattice

All the networks discussed above are based on two-dimensional lattices. Similar results can also be shown in the context of a one-dimensional version of the communication network of nodes and hubs. The base network is a ring lattice of size L with nearest-neighbor interaction. Hubs are distributed randomly in the lattice where each hub has $2k$ nearest neighbors [Fig. 1(c)]. As in the 2D lattice no two hubs are separated by a less than a minimum distance, $d_{\min}=1$. In our simulation we have taken $k=4$ although Fig. 1(c) illustrates only $k=2$ connections. The distance between a source and target is defined by the Manhattan distance $D_{st}=|is-it|$. If a message is routed from a source S to a target T on this lattice through the baseline mechanism, it takes the path $S-1-2-Y-3-4-5-T$ as in Fig. 1(c). The routing algorithm is same as that used in the 2D model [7,8]. A given number N_m of source and target pairs start sending N_m messages continuously at every 100 time steps for a total run time of 30 000. The plot of $N(t)$ as a function of time t for this lattice [Fig. 2(c)] attains saturation for $t \simeq 10^8$.

The travel time is calculated for a source-target separation of $D_{st}=2000$ on a $L=10\,000$ ring lattice and averaged over 1000 hub realizations. For the baseline mechanism, where network congests at these values, the data for travel time distribution can be fitted by a Gaussian [Fig. 8(a)]. If the hubs are connected by the assortative mechanism, all the messages are cleared, and the distribution can be fitted well by a logarithmic-normal function with a power-law correction of the form

$$P(t) = \frac{1}{t\sigma\sqrt{2\pi}}\exp\left(-\frac{(\ln t-\mu)^2}{2\sigma^2}\right)(1+Bt^{-\delta}), \qquad (4)$$

as shown in Fig. 8(b).

Thus if the hubs are connected by assortative mechanisms, there is no congestion, and the leading behavior is logarithmic normal as in the decongested case of the 2D networks. An additive power-law correction is seen due to the 1D nature of the network. Due to the ring geometry of the network, some messages are not routed through the links created due to the assortative connections between hubs. These messages thus have larger travel times and contribute additive power-law corrections to the basic logarithmic-normal behavior in the decongested phase.

C. Stochastic process for transport

It is clear that the displacement of a message on the network depends on factors that are partly systematic, and

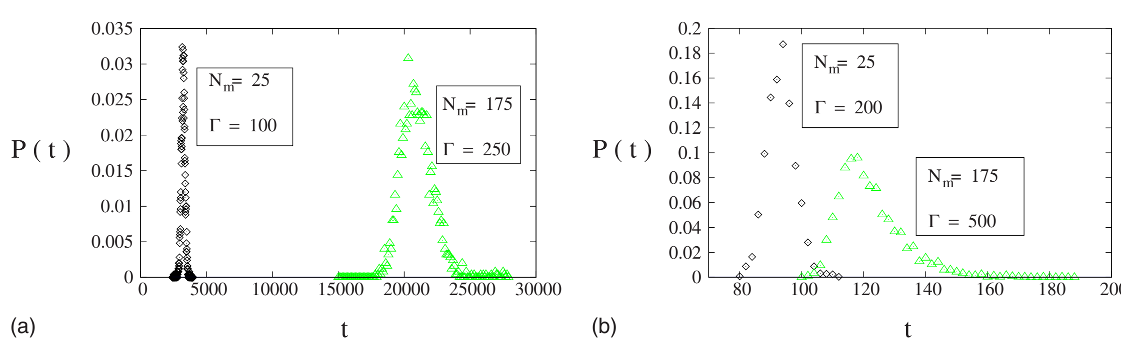

FIG. 7. (Color online) The plot of travel time distribution of messages shows (a) Gaussian distribution in the congested phase for $N_m=25$, $\Gamma=100$ ($\sigma=129$) and $N_m=175$, $\Gamma=250$ ($\sigma=1147.08$) and (b) logarithmic-normal behavior in the decongested phase for $N_m=25$, $\Gamma=200$ ($\sigma=0.0484$) and $N_m=175$, $\Gamma=500$ ($\sigma=0.0668$). The lattice is the baseline lattice.

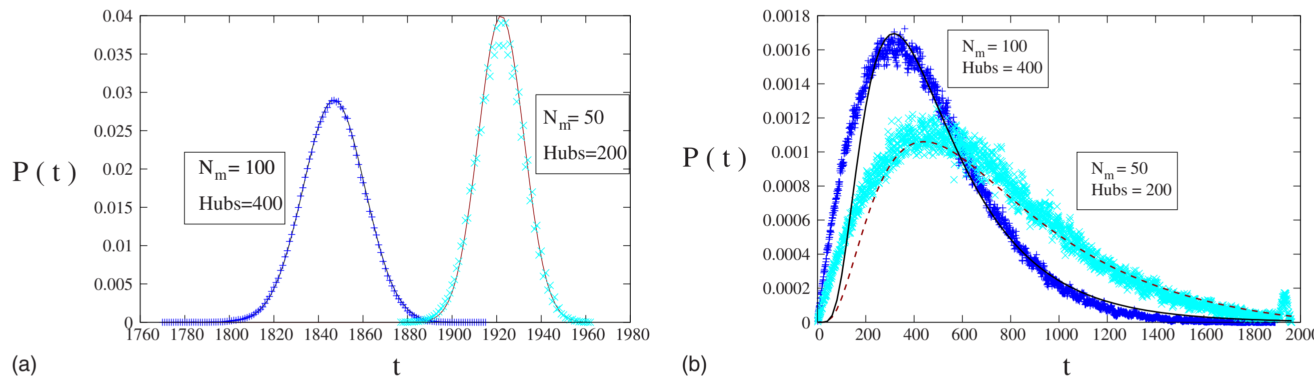

FIG. 8. (Color online) The plot of travel time distribution of messages for the 1D ring lattice shows (a) Gaussian distribution in the congested phase. The standard deviation σ is (*i*) 13.86 (χ^2=0.0086) for N_m=100 and 400 hubs (*ii*) 10.21 (χ^2=0.0095) for N_m=50 and 200 hubs. (b) Logarithmic-normal behavior with a power-law correction is seen in the decongested phase. (*i*) N_m=100 and 400 hubs, σ=1.42 (χ^2=0.14), β=0.88, B=−0.0009 and (*i*) N_m=50 and 200 hubs, σ=1.79 (χ^2=1.75), δ=0.91, B=−0.0009.

partly random, with the random element arising due to interference from other messages and limitations of hub capacity. Hence, message transfer in both the congested and decongested phases can be modeled by stochastic differential equations. In the congested phase, the displacement X_t of the message at a time t can be modeled by the equation

$$dX_t = \mu(X_t)dt + \sigma(X_t)dW_t. \tag{5}$$

Here, $\mu(X_t)$ represents the drift coefficient, $\sigma(X_t)$ is the diffusion coefficient and W_t is a Wiener process. The probability distribution $f(X,t)$ satisfies the forward Kolmogorov equation

$$\frac{\partial f}{\partial t} = \frac{[\partial\mu(X)f(X,t)]}{\partial X} + \frac{\partial^2}{\partial X^2}[\sigma^2(X)f(X,t)]. \tag{6}$$

The stationary solution, i.e., $\frac{\partial f}{\partial t}=0$ can be found using Wright's formula [16]

$$f(x) = \frac{N}{\sigma^2}\int_{-\infty}^{x}\frac{\mu(s)}{\sigma^2(s)}ds, \tag{7}$$

where N is a normalization constant and μ and σ are the drift and diffusion coefficient defined above. If the drift coefficient is of the form $\mu(X_t)=(\bar{\mu}-X_t)$ and the diffusion coefficient $\sigma(X_t)$ is a constant, then, the stationary probability distribution $f(X)$ turns out be of the normal form

$$f(x) = \frac{1}{\sigma\sqrt{2\pi}}\exp - \frac{(X-\bar{\mu})^2}{2\sigma^2}. \tag{8}$$

On the other hand, in the decongested phase, the process can be modeled by the equation

$$dX_t = \mu(X_t)X_t dt + \sigma X_t dW_t. \tag{9}$$

Now if we define $S(X)=\log(X)$, then Eq. (9) can be rewritten in terms of the variable $S(x)$ and reduced to the form of Eq. (5). Then, using the transformation $f(X)=f(S)\frac{dS}{dX}$, we find the form of $f(X)$ in the decongested phase to be of the logarithmic-normal form

$$f(X) = \frac{1}{\sigma X\sqrt{2\pi}}\exp - \frac{(\ln X-\bar{\mu})^2}{2\sigma^2}. \tag{10}$$

Here, we assume the drift and diffusion constants to have the same forms as in the congested phase. Thus, the stochastic equation in the congested phase is governed by a stochastic process of the Brownian type, whereas that in the decongested phase is governed by a process of the geometric Brownian type. We note that the behavior in the decongested phase has been modeled earlier by a geometric Brownian process in Ref. [17], and the resulting logarithmic-normal distributions have been compared with the internet latencies. The latencies or travel times are directly proportional to the displacements. Thus the normal and logarithmic-normal distributions of the travel times in the congested and decongested phases have the forms in Eqs. (8) and (10). The change in the nature of the distribution arises from the fact that the nature of the noise is different in the two phases, being linear multiplicative in the decongested phase and additive in the congested phase. Our analysis is valid in arbitrary dimensions.

IV. CONCLUSION

To summarize, the statistical characterizers of the communication networks studied here, viz. the travel time distributions show the characteristic signatures of the congested or decongested state of the network being normal in the congested phase and logarithmic normal in the decongested phase. The results are true for the locally clustered communication network as well as the Waxman topology network and also carry over to a one-dimensional lattice to leading order. Thus the travel time distribution is a robust characterizer of the congested or decongested phase. For the 1D lattice, the distribution carries an additional signature of the topology in the form of an additive power-law correction to the leading order. The waiting time distributions carry identical signatures of the congested and decongested phase. These results are valid for different lattice sizes and hub densities as well [18]. The displacement of the message can be modeled by stochastic equations with linear drift. The noise term in the equation is additive in the congested phase and linear multiplicative in the decongested phase, leading to the normal and logarithmic-normal distributions observed in the congested and decongested phases.

We note that model networks based on two-dimensional geometries considered by other authors have been observed to show congestion-decongestion transitions [10,11,19]. It has also been noted that the nature of the congestion transition depends on the type of routing rules [20] which also affect network performance and traffic fluctuations [21,22]. Minimal models of traffic flow utilizing random walks have also been proposed [23]. We hope to explore the utility of our characterizers for these phase transition situations in future work.

Finally, several two-dimensional model networks demonstrate traffic characteristics similar to those seen for the internet [11,24]. Additionally, networks that incorporate geographic clustering and encounter congestion problems arise in many practical situations e.g., cellular networks [25] and air traffic networks [26]. Logarithmic-normal latencies have been associated with the decongested phase of the internet and have been analyzed using stochastic models [17]. Our results can therefore have relevance in real life contexts.

ACKNOWLEDGMENTS

We thank CSIR, India for support under their extramural scheme. N.G. thanks V. Balakrishnan for useful discussions and for reading the paper.

[1] B. Tadic, G. J. Rodgers, and S. Thurner, Int. J. Bifurcat. Chaos Appl. Sci. Eng. **17**, 2363 (2007).
[2] J. J. Wu, Z. Y. Gao, H. J. Sun, and H. J. Huang, Europhys. Lett. **74**, 560 (2006).
[3] T. Nagatani, J. Phys. Soc. Jpn. **62**, 2533 (1993).
[4] T. L. Olsen, Oper. Res. Lett. **28**, 113 (2001).
[5] S. H. Kang, D. K. Sung, and B. D. Choi, IEEE Commun. Lett. **2**, 17 (1998).
[6] B. M. Waxman, IEEE J. Sel. Areas Commun. **6**, 1617 (1988).
[7] B. K. Singh and N. Gupte, Phys. Rev. E **71**, 055103(R) (2005).
[8] S. Mukherjee and N. Gupte, Phys. Rev. E **77**, 036121 (2008); Pramana **70**, 1109 (2008).
[9] J. Kleinberg, Nature (London) **406**, 845 (2000).
[10] T. Ohira and R. Sawatari, Phys. Rev. E **58**, 193 (1998).
[11] S. Valverde and R. V. Sole, Physica A **312**, 636 (2002).
[12] A. Lakhina, J. W. Byers, M. Crovella, and I. Matta, IEEE J. Sel. Areas Commun. **21**, 934 (2003).
[13] S. Verma, R. K. Pankaj, and A. Leon-Garcia, Perform. Eval. **34**, 273 (1998).
[14] Networks can congest even with a one time deposition of messages, if the number of messages is sufficiently high. All the subsequent discussion here is applicable for this case as well.
[15] The CBC of the mth hub is defined as the ratio $CBC = N_m/N$, where N_m is the number of messages that pass through the hub m and N is the total number of messages running on the lattice.
[16] L. Cobb, *Mathematical Frontiers of the Social and Policy Sciences*, by L. Cobb and R. M. Thrall (Westview, Colorado, 1981), Chap. 2.
[17] B. A. Huberman and R. M. Luckose, Science **277**, 535 (1997).
[18] We observed similar behavior for (i) $L=5000$, $N_m=50$, $D_{st}=1000$, and 200 hubs and (ii) $L=20\,000$, $N_m=200$, $D_{st}=4000$, and 800 hubs for the 1D lattice.
[19] G. Mukherjee and S. S. Manna, Phys. Rev. E **71**, 066108 (2005).
[20] P. Echenique, J. Gomez-Gardenes, and Y. Moreno, Europhys. Lett. **71**, 325 (2005).
[21] B. Tadic, S. Thurner, and G. J. Rodgers, Phys. Rev. E **69**, 036102 (2004); G. Yan, T. Zhou, B. Hu, Z.-Q. Fu, and B.-H. Wang, *ibid.* **73**, 046108 (2006).
[22] M. A. de Menezes and A.-L. Barabasi, Phys. Rev. Lett. **92**, 028701 (2004); J. Duch and A. Arenas, *ibid.* **96**, 218702 (2006).
[23] D. De Martino, L. Dall'Asta, G. Bianconi and M. Marsili, Phys. Rev. E **79**, 015101(R) (2009).
[24] M. Takayasu, H. Takayasu, and T. Sato, Physica A **233**, 824 (1996).
[25] H. Jeong, S. P. Mason, Z. N. Oltvai, and A. L. Barabasi, Nature (London) **411**, 41 (2001).
[26] C. Mayer and T. Sinai, Am. Econ. Rev. **93**, 1194 (2003).